Conformational transitions in a lattice model of a three-component mixture of solvent, amphiphile, and soluble polymers

D. E. Jennings, Yu. A. Kuznetsov, E. G. Timoshenko, and K. A. Dawson[a)]
Irish Centre for Colloid Science and Biomaterials,[b)] Department of Chemistry, University College Dublin, Belfield, Dublin 4, Ireland

(Received 23 May 1997; accepted 16 October 1997)

We present a lattice model of amphiphile, solvent and polymer. The model is simulated in a hybrid Monte Carlo scheme using the grand canonical ensemble for solvent and amphiphile, and the canonical ensemble for the polymer. The model has been studied for a limited range of parameters, albeit consistent with the most elementary properties of surfactants and polymer. However, despite this apparently very simple set of microscopic interactions, a number of concentration-dependent effective interactions emerge, and cause conformational transitions of the polymer. We examine surfactant-polymer binding curves to relate these conformational changes of the polymer to binding. We have established the viability of using Monte Carlo simulations to study solutions of amphiphile, polymer and solvent. © *1998 American Institute of Physics.* [S0021-9606(98)51304-9]

I. INTRODUCTION

In the late 1980s and early 1990s numerous researchers focused on models of self assembly relevant to amphiphile-water[1–4] and amphiphile-oil-water mixtures.[5–8] Considerable advances were made in experiment,[9–11] simulation[12–17] and theory[5,18–23] and the connections between them.[24–26] Simultaneously, much of the basic intellectual infrastructure to understand solutions of polymers (see, e.g., Refs. 27–30, and references therein) was developed and careful comparisons to experiment were made.[31,32]

Recent experimental interest has tended more toward mixtures of amphiphile-polymer and solvent, as evidenced by work in synthetic polymers[33–41] and biopolymers.[42–51] The reasons are, in part, that many of the most important practical questions from the food, cosmetics, pharmaceutical and other industries revolve around these types of mixtures, the classical oil-water-amphiphile systems having been mainly the preserve of the oil industry. This trend will undoubtedly grow. It is our opinion that elegant science is emerging from studies of these novel systems.

In this paper we intend to show that a lattice model may be adapted to permit the study of these ternary mixtures.

II. MODEL AND METHOD

In this model of ternary mixtures containing polymers, amphiphile and solvent the degree of polymerisation (N) and concentration of the polymer (ϕ_c) are fixed, whereas the number of solvent and amphiphile particles may vary. The polymer is therefore treated within the canonical ensemble (T,V,N) and the solvent and amphiphile molecules within the grand canonical ensemble (T,V,μ). It is worth noting at this point that when we use the term solvent we normally have water in mind. However, as with all such lattice models, there is no real specification of the solvent as water, except via the interactions. In any case, we may for our present purpose use ''water'' and ''solvent'' interchangeably, providing these issues are borne in mind.

The simulation consists of a variety of Monte Carlo moves. Those controlling the movements of the polymer are the conventional local bond movements and reptation[29,52] while those dealing with solvent and amphiphile particles are of conventional spin-flip type. There are two main relaxation times in this model, one for amphiphile and solvent molecules, τ_{latt}, and the other for the polymer chain τ_{poly}. The characteristic relaxation time for a single spin grand canonical ensemble is $\tau_{latt}=S^2$, where S is the lattice size. τ_{poly} is the relaxation time of a connected object and should scale roughly as N^2 where local moves dominate (as in dilute solutions) and N^3 for reptation, where N is the length of the polymer.

All of these issues, as well as the normal practices of computer simulation are taken into account in our work, though we do not emphasize the technicalities in this presentation. One point however is worth making. Thus, the presence of the amphiphile, and also the possibility of conformational collapse has been found to require reptation moves in even dilute polymer systems, in contrast to previous studies. Without attention to such issues it is rather hard to find many of the transitions discussed here. Naturally we have checked that the presence of the transitions is unaffected by changing the balance between the different types of move—a property of the state of equilibrium, within the obvious constraint that reptation is a significant and important move through the range of polymer concentration.

We consider a simple lattice model of three-component mixtures. The Hamiltonian for a polymer-water-amphiphile system is comparable to that of oil-water-amphiphile models,[18,19] but with the addition of polymer molecules replacing the oil.[29] A particular expression of this type of model is given by the effective Hamiltonian,

[a)]Author to whom all correspondence should be addressed.
[b)]Established at Queens University Belfast and University College Dublin.

$$H_\mu \equiv H - \sum_i \mu_{s_i} \equiv H - (\mu_s N_s + \mu_a N_a), \tag{1}$$

$$H = -\sum_{\langle ij \rangle} w(r_{ij}) I_{s_i s_j} - \sum_{(ijk)} I_{s_i s_j s_k}, \tag{2}$$

where i,j,k enumerate the lattice sites, and s_i denotes the contents of the ith site. Each site may be occupied by a monomer (m), solvent (s) or amphiphile (a) molecules and vacancies are not admitted. The chemical potential μ_{s_i} can take on three possible values μ_a, μ_s or zero depending on whether the site i is occupied by an amphiphile, a solvent molecule or by a monomer. Here N_a and N_s are the total number of amphiphile and solvent sites, respectively, such that $N_a + N_s + N = S^3$, with S being the linear size of the lattice.

$I_{s_i s_j}$ is a 3×3 symmetric matrix of two body interactions representing the monomer-monomer I_{mm}, monomer-solvent I_{ms}, monomer-amphiphile I_{ma}, solvent-solvent, I_{ss}, solvent-amphiphile, I_{sa} and amphiphile-amphiphile, I_{aa}, interaction constants, respectively. The notation (ijk) indicates a sum over all sets of three sites in a row. The term $I_{s_i s_j s_k}$ may take three values; $+L$ for monomer-amphiphile-solvent (I_{mas}) and solvent-amphiphile-monomer (I_{sam}) interactions, $-L$ for monomer-amphiphile-monomer (I_{mam}) and solvent-amphiphile-solvent (I_{sas}) interactions, and zero otherwise. The distance between sites i and j is denoted as $r_{ij} = |\vec{r}_i - \vec{r}_j|$ and $w(r_{ij})$ is a function with the property $w(b) = 1$, where b is the lattice spacing. Short range interactions are introduced by setting $w(r) = 0$ for $r > R_{max}$, where $R_{max} = 2b$ in our case. Each site interacts with its nearest neighbors $(r_{ij} = b; w(b) = 1.0)$, diagonal neighbors $(r_{ij} = \sqrt{2b}; w(\sqrt{2b}) = 1.0)$, long-diagonal neighbors $(r_{ij} = \sqrt{3b}; w(\sqrt{3b}) = 0.75)$ and next-nearest neighbors $(r_{ij} = 2b; w(2b) = 0.5)$. See Ref. 29 for more details. We note, however, that here use is made of periodic rather than reflective boundary conditions to improve equilibration properties. We shall use the units of measurement in which the lattice spacing, $b = 1$ and $k_B T = 1$.

Local internal moves and reptations are used to update the polymer conformation. Both use a special method, determined by the structure of the Hamiltonian, to generate neighborhood polymer structures while maintaining polymer connectivity and excluded volume constraints. There are two types of elementary polymer moves: those involving the pairs polymer-solvent and polymer-amphiphile. The simplest example of an elementary monomer move for a two-dimensional (2D) lattice is presented in Figure 1 where $\times$ represents either a solvent or amphiphile molecule that is to be exchanged for a monomer. In this case, for nearest-neighbor interactions only $(R_{max} = b)$, the energy difference between the final and initial states for a monomer-solvent move ΔE_{m2s} and a monomer-amphiphile move ΔE_{m2a} is

$$\Delta E_{m2s} = 2I_{ms} - I_{mm} - I_{ss}, \tag{3}$$

$$\Delta E_{m2a} = I_{ms} + I_{ma} - I_{mm} - I_{as}. \tag{4}$$

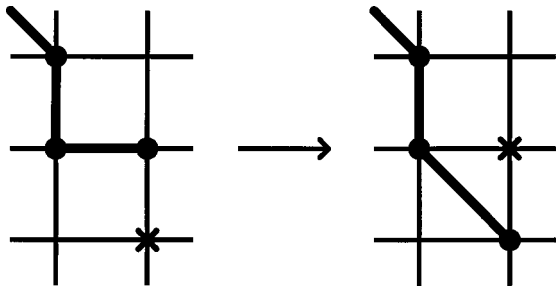

FIG. 1. An example of elementary monomer move on 2D lattice, where $\times$ represents either a solvent or amphiphile molecule that is to be exchanged for a monomer.

For a ternary system, one has to take into account the change in energy due to the three-body interactions as well as that due to the two-body interactions. A monomer-solvent or a monomer-amphiphile attempted move is accepted or rejected based on the METROPOLIS ratio of the transition probabilities η_{m2s} and η_{m2a}, respectively,

$$\eta_{m2s} = \exp\left(\frac{-\Sigma_r w(r)\Delta E_{m2s}(r) - \Delta E_L}{k_B T}\right), \tag{5}$$

$$\eta_{m2a} = \exp\left(\frac{-\Sigma_r w(r)\Delta E_{m2a}(r) - \Delta E_L}{k_B T}\right), \tag{6}$$

where the summation is over all the neighboring sites with $w(r) > 0$. $\Delta E_{m2s}(r)$ is the difference in the the two-body interaction energy between the final and initial states at each interaction distance, r. ΔE_L is the difference in the three-body interaction energy between the final and initial state. $E_L(x)$, the three-body interaction energy of site x in a row of sites $vwxyz$, is calculated by summing the terms $I_{s_v s_w s_x}$, $I_{s_w s_x s_y}$ and $I_{s_x s_y s_z}$. For example, if the contents of the sites $vwxyz$ are amphiphile-amphiphile-monomer-amphiphile-solvent, then $E_L(x) = I_{aam} + I_{ama} + I_{mas} = L$.

The elementary spin-flip of a solvent to an amphiphile is accepted with the METROPOLIS ratio of the transition probability η_{s2a}. The METROPOLIS ratio of the transition probability for a spin-flip of an amphiphile to a solvent η_{a2s} is the reciprocal of η_{s2a}. Thus

$$\eta_{s2a} = \exp\left(\frac{-\Sigma_r w(r)\Delta E_{s2a}(r) - \Delta E_L - \mu}{k_B T}\right), \tag{7}$$

$$\eta_{a2s} = \eta_{s2a}^{-1}, \tag{8}$$

where the summation is again over all the neighboring sites with $w(r) > 0$ and $\Delta E_{s2a}(r)$ is the difference in the two-body interaction energy for a solvent to amphiphile spin-flip between the final and initial states at each interaction distance, r. The model defined by Eq. (1) in the grand canonical ensemble for amphiphile and solvent and in the canonical one for the polymer obviously depends only on the relative chemical potential, $\mu \equiv \mu_a - \mu_s$. We see that replacing μ_{s_i} by $\mu_{s_i} - \mu_s$ in Eq. (1) to exclude μ_s from consideration results in a trivial constant shift $H_\mu \rightarrow H_\mu + \mu_s(S^3 - N)$, that does not affect the thermodynamics.

It may be shown that the model[8] depends only on the following combinations of two-body interaction parameters $I_{s_i s_j}$:

$$\chi_{m-m2s}=2I_{ms}-I_{mm}-I_{ss},$$
$$\chi_{a-m2s}=I_{ms}+I_{as}-I_{ma}-I_{ss},$$
$$\chi_{m-m2a}=I_{ms}+I_{ma}-I_{mm}-I_{as},$$
$$\chi_{a-m2a}=I_{ms}+I_{aa}-I_{ma}-I_{as},$$
$$\chi_{m-s2a}=I_{ms}-I_{ma},$$
$$\chi_{a-s2a}=I_{as}-I_{aa}, \tag{9}$$
$$\chi_{s-s2a}=I_{ss}-I_{as}.$$

which are in units of k_BT. Equations (5)–(8) for the METROPOLIS ratio of transition probabilities are rearranged in terms of interaction parameters and the difference in the number of neighboring monomers, solvent molecules and amphiphiles:

$$\eta_{m2s}=\exp\left(\frac{\chi_{m-m2s}\Sigma_r w(r)\Delta n_m(r)+\chi_{a-m2s}\Sigma_r w(r)\Delta n_a(r)-\Delta E_L}{k_BT}\right), \tag{10}$$

$$\eta_{m2a}=\exp\left(\frac{\chi_{m-m2a}\Sigma_r w(r)\Delta n_m(r)+\chi_{a-m2a}\Sigma_r w(r)\Delta n_a(r)-\Delta E_L}{k_BT}\right), \tag{11}$$

$$\eta_{s2a}=\exp\left(\frac{\chi_{m-s2a}\Sigma_r w(r)\Delta n_m(r)+\chi_{a-s2a}\Sigma_r w(r)\Delta n_a(r)}{k_BT}+\frac{\chi_{s-s2a}\Sigma_r w(r)\Delta n_s(r)-\Delta E_L-\mu}{k_BT}\right), \tag{12}$$

where the summation is over all the neighboring sites with $w(r)>0$ and $\Delta n_m(r)$ is the difference in the number of monomers between the final and initial states at each interaction distance, r. Likewise, $\Delta n_a(r)$ and $\Delta n_s(r)$ are, respectively, the difference in the number of amphiphiles and the number of solvent molecules between the final and initial states at each interaction distance, r.

It is clear that, as with all of these types of lattice models, there are a number of parameters that must be fixed in order to reflect the common experimental regimes. However, in this paper we intend mainly to show that the model may be simulated, and that a number of interesting physical phenomena are present for the simplest choices of interactions. In our discussion all the couplings in Equation (9) are zero, only the three-body interaction parameter, $I_{s_i s_j s_k}$, is non-zero.

Of course, there are still connectivity and excluded volume constraints for the polymer which are taken into account explicitly. If the amount of amphiphile is small, arranged by the appropriate choice of μ we would recover in this case a self-avoiding random walk for the chain producing the Flory exponent of the Flory coil, $V\approx\frac{3}{5}$.[29,30] It is quite interesting to see how the presence of the amphiphile would affect the system via the three-body interactions. That will be the main subject of our current study. In practice this has the following implications. Only three independent triplet arrangements of polymer monomers (m), amphiphile (a), and solvent (s) have non-zero three-body interactions. The linear triplets (mas) have the favorable energy $+L$, while the others, (mam) and (sas) are both unfavorable with energy $-L$. Equations (9)–(11) for the METROPOLIS ratio of the transition probabilities ($\eta_{m2s},\eta_{m2a},\eta_{s2a}$) reduce to

$$\eta_{m2s}=\eta_{m2a}=\exp\left(\frac{-\Delta E_L}{k_BT}\right), \tag{13}$$

$$\eta_{s2a}=\exp\left(\frac{-\mu-\Delta E_L}{k_BT}\right), \tag{14}$$

$$\eta_{a2s}=\eta_{s2a}^{-1}. \tag{15}$$

Note that this choice of interaction parameters has the direct tendency to favor amphiphile binding to the polymer, and the indirect tendency to favor micelle formation relative to isolated amphiphile in solvent. This seems to be a sensible place to begin our studies. For polymer-amphiphile-solvent systems we will exhibit results for a variety of values of the effective three-body interaction constant, $l=L/k_BT$, over a range of amphiphile-solvent concentrations. Despite this apparently very simple set of microscopic interactions, a number of concentration-dependent effective interactions emerge, and cause conformational transitions of the polymer. This is a motif that we shall seek to emphasize in our current presentation.

Finally, let us comment on the way physical quantities are calculated. For a given set of the model parameters (such as l,μ,N,S and so on) using the hybrid METROPOLIS algorithm we produce a large set of Q statistically independent configurations of the system by equilibrating different initial states. Any physical observable, A, discussed below is obtained as a statistical average which is approximated by the formula,[53]

$$\langle A\rangle\approx\frac{1}{Q}\sum_{i=1}^{Q}A_i, \tag{16}$$

where A_i are the values of this observable for the ith member of the set of Q statistically independent configurations. Typically $Q\approx 10^3,10^4$.

III. RESULTS AND DISCUSSION

We shall make no attempt to exhaustively analyze the many-dimensional phase diagram of this model and concentrate instead on the l term mediated conformational transitions for the polymer. We have carried out extensive calculations for a variety of chain lengths, $N=20,40,80$ at three values of $l=L/k_BT=1.0$, 1.66 and 5.0. Some calculations with $N=100$ for $l=1.35,1.4,1.45$ have also been carried out. These investigations have been made for lattice size, $S=20$, and mostly the dilute polymer limit in which only one chain is present in that volume. The chain volume fraction is therefore $\phi_c=M/S^3=1/20^3$, where M is the number of polymer chains and S^3 is the volume of the box. In addition we have, for $N=40$, made preliminary investigations of a chain concentration that is closer to the pure polymer semidilute regime, $\phi_c=10/20^3$, in order to exhibit the feasibility of our study.

One reason for focusing on the very dilute limit is to permit a clear discussion of such phenomena as amphiphile-polymer binding curve, in the absence of inter-polymer effects, the subject of much recent experimental work.[43,45,48,54–59] In our binding curve work we consider only the lowest range of free amphiphile concentration to avoid complications of more extended bound clusters. This issue will be revisited in a later publication. We shall plot $\beta=\langle n_b\rangle/n_{bs}$ versus c_f, the mean volume fraction of free amphiphile, as this is the typical quantity emerging from amphiphile selective electrode measurements (see, e.g., Refs. 48 and 60–63 and references therein). Here n_{bs}, the number of available binding sites for a polymer, is constant as a binding site is defined as a site that is within an interaction distance $r<2$ of a monomer molecule ($n_{bs}=26$). Also, n_b is the number of amphiphiles bound to a polymer or the number of occupied binding sites for a polymer. Correspondingly c_b is the mean volume fraction of bound amphiphile, c_f is the mean volume fraction of free amphiphile and c_t is the mean volume fraction of total amphiphile, $c_t=c_b+c_f$. We will be able to compare this data to calculated heat capacities, C_V/k_B, and the polymer radius of gyration, R_g, which are defined as

$$\frac{C_V}{k_B}=\frac{1}{(k_BT)^2}(\langle H^2\rangle-\langle H\rangle^2),$$
$$R_g^2=\left\langle\frac{1}{2N^2}\sum_{nn'}(\vec{r_n}-\vec{r_{n'}})^2\right\rangle, \tag{17}$$

where H is defined in Eq. (2) and $\vec{r_n}$ are the coordinates of the nth monomer along the chain. This will enable one to connect binding to the conformational transitions of the polymer. In Figure 2 we relate the relative chemical potential to concentration by plotting μ versus c_t, the mean volume fraction of amphiphile.

We begin by examining the heat capacity, C_V/k_B, plotted against μ for $N=20$ (Figure 3), where only the strongest polymer conformational transitions are visible. For $l=1.0(\bigcirc)$ there is a simple broad maximum (peak B) corresponding to a type of amphiphile-solvent phase separation.

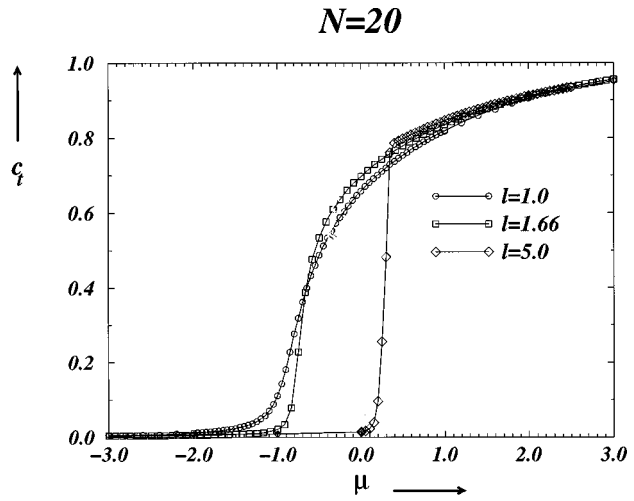

FIG. 2. Plot of the mean volume fraction of amphiphile, c_t versus μ, the relative chemical potential for $N=20$, $l=1.0(\bigcirc)$, $l=1.66(\square)$ and $l=5.0(\diamond)$.

The polymer partitions into the surfactant phase, and we note the combination of attraction of amphiphile to polymer and effective amphiphile-amphiphile attractions tends to stretch the polymer (Figure 4) implying that the amphiphile rich phase is a good solvent for this choice of parameters.

For $l=1.66(\square)$ and $N=20$, we note the emergence of two new phenomena at $\mu\approx-3.4$ (peak A) and at $\mu\approx+3.4$ (peak C). Possibly these transitions are symmetry related but as we shall see, not in any simple manner. A similar pattern of transitions has been observed for $l=5.0$ also. Comparison of R_g (Figure 4) and other observables indicates that peak A corresponds to a strong shrinkage of the polymer chain. Examination of the configuration for $N=20$ as well as much larger chains ($N=40,80$), where the phenomenon persists and becomes more pronounced, indicates that the chain forms a *platelet* structure. We exhibit a sample conformation for $N=40$ and $N=80$ (Figure 5). The reason for the collapse

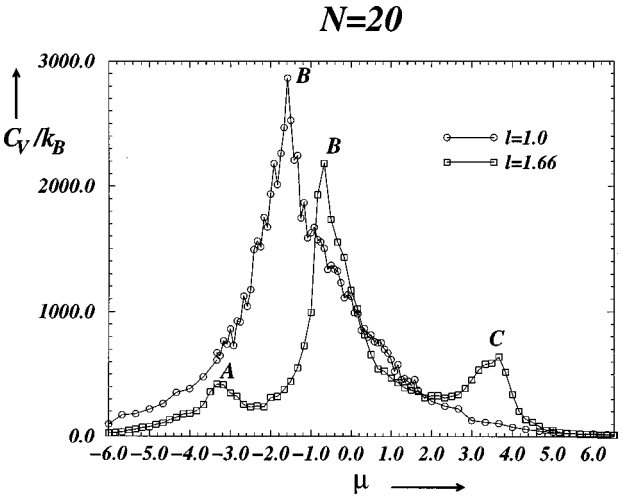

FIG. 3. Plot of the heat capacity, C_V/k_B, versus μ for $N=20$, $l=1.0(\bigcirc)$ and $l=1.66(\square)$. Each peak is labelled A, B and C to facilitate discussion of phase transitions in the text.

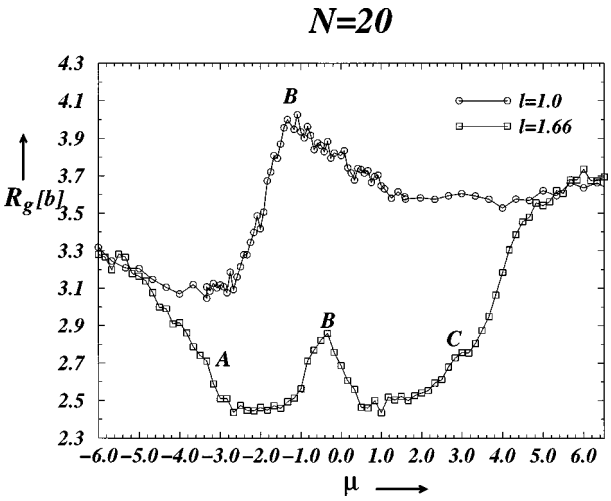

FIG. 4. Plot of the polymer radius of gyration, R_g, versus μ for $N=20$, $l=1.0$(○) and $l=1.66$(□). A, B and C correspond to peaks in the heat capacity, C_V/k_B, for the same parameters.

is that some amphiphile has bound to the polymer because of the favorable (mas) interaction. However, the consequence is, especially for an incompletely covered chain, a number of unfavorable (sas) interactions arise. As the amphiphile concentration increases the system ultimately finds the means to minimize the unfavorable (sas) interactions and maximize the favorable (mas) interactions by collapsing into a *platelet* structure shown in Figure 5. In brief then, the amphiphile is binding to the polymer with the head-group strongly attached to the polymer. The result is that amphiphile tails are exposed to solvent and avoid this by collapse. We accept that the choice of interactions we have made is quite limited and the details of the collapsed structures would need to be examined further. However, we have at least an analogy of the phenomena observed when, for example, giant DNA collapses in the presence of cationic lipids.[64]

Consider again Figures 3 and 4. For $N=20$ and $l=1.66$ as we pass through peak B there is at first sufficient amphiphile to disrupt the *platelet* and, as for $l=1.0$, the amphiphile behaves as a good solvent leading to expansion of the chain. However, remarkably, beyond peak B we see another collapse where the system is amphiphile rich. In such a case with much amphiphile and only a little solvent, the only way to preserve the favorable monomer-amphiphile-solvent interactions is a *sandwich* structure such as that exhibited for $N=80$ in Figure 6. Note the remarkable emergence of effective concentration dependent interactions. Now, beyond peak C we return finally to the amphiphile dense regime where the polymer is fully expanded as it is essentially experiencing a good solvent. All the comments we have made for $N=20$ are equally relevant for our observations of $N=40,80$ at $l=1.0,1.66,5.0$, though the phenomena become more pronounced, and transitions sharper with increasing chain length. In Figure 7, we show the heat capacity for chains of $N=40$ at $l=1.66$.

We will not yet attempt to present even the low polymer concentration cut of the phase diagram since more extensive

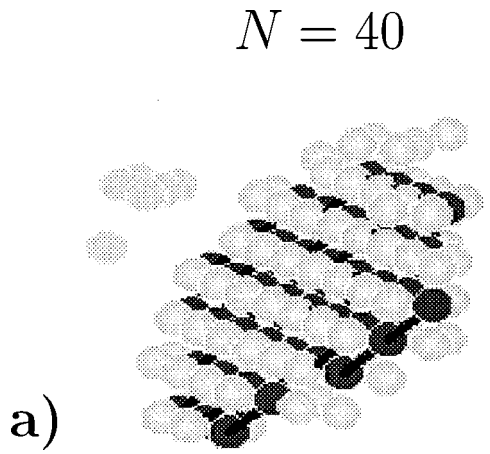

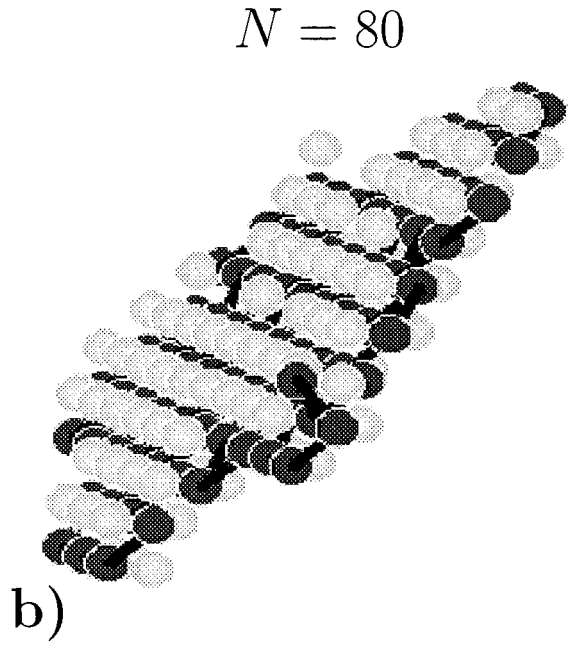

FIG. 5. Visual representation of the collapsed polymer *platelet* structure formed beyond peak A for $l=1.66$, $N=40$ (a) and $N=80$ (b). This is a very dilute solution of amphiphile and polymer in the solvent-rich phase. Solvent is represented as (white), amphiphile (gray) and polymer (dark gray/black).

calculations would be required. However, the overall scheme has already begun to emerge. As the concentration of amphiphile increases there is a simple phase separation between water-rich and amphiphile-rich phase, a transition that would terminate in a critical point as the temperature increases. However, buried within this, for lower temperatures ($l>1$) there are two polymer conformational transitions at very low polymer concentrations. These are not macroscopic phase transitions, in the same sense that simple single chain collapse is not a phase transition. However for high polymer concentrations this situation may change.

Let us now turn to the binding of amphiphile to the

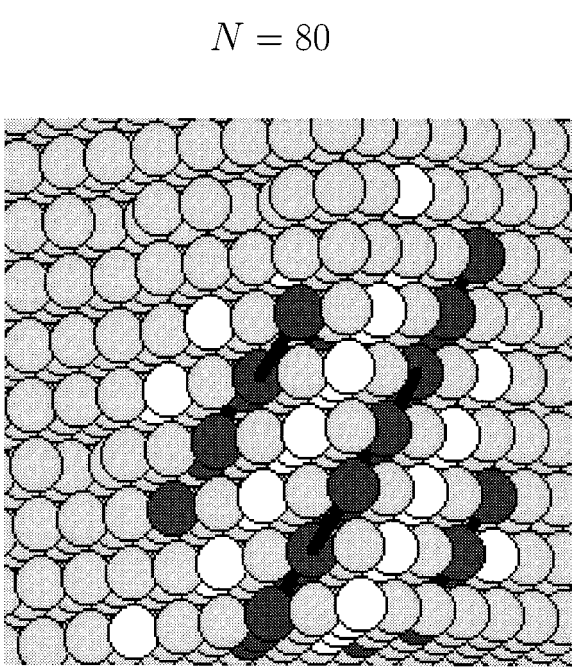

FIG. 6. Visual representation of part of the collapsed polymer *sandwich* structure for $N=80$, $l=1.66$. The sandwich structure forms after peak B in the amphiphile-rich phase with only a small number of solvent molecules present. This structure preserves the favorable monomer-amphiphile-solvent interactions. Solvent is represented as (white), amphiphile (gray) and polymer (dark gray/black).

chain. Again, we emphasize that no more than preliminary results are offered. We present binding curves β versus c_f for very low amphiphile concentrations for $N=20$, $l=5.0,1.66,1.0$ in Figure 8 and $N=100$, $l=1.35,1.45,1.66$ in Figure 9. We point out that the range of chemical potentials for which we here present results is much lower than that of interest in studying the full range of conformational transitions.

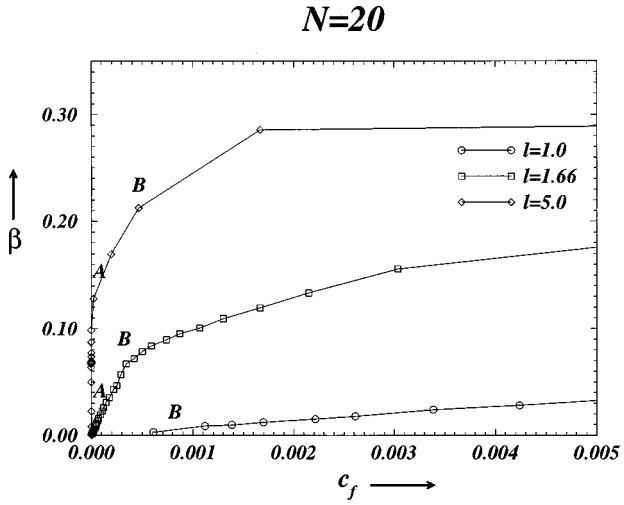

FIG. 8. Plot of the amphiphile-polymer binding curves, β versus c_f, for $N=20$, $l=1.0(\bigcirc)$, $l=1.66(\square)$, $l=5.0(\diamond)$. Here $\beta=\langle n_b\rangle/n_{bs}$, where n_b is the number of amphiphiles bound to a polymer, and n_{bs}, the number of available binding sites for a polymer, is constant as a binding site is defined as a site that is within an interaction distance $r<2$ of a monomer ($n_{bs}=26$). c_f is the mean volume fraction of free amphiphile. A and B correspond to peaks in the heat capacity for the same parameters.

Indeed, we have shown only results where the effective amphiphile chemical potentials lie in the range $\mu<-2.0$, and typically, there would then be only sufficient amphiphile to cover all of the polymers available sites. In Figure 8 we see that the binding occurs in a relatively uncooperative fashion, saturating finally at higher ambient amphiphile concentrations. The behavior of β is at first relatively linear at low c_f. Also, for larger l, the slope is larger reflecting the fact that most of the added amphiphile is adsorbed to the polymer, and little is available as free amphiphile. In Figure 8 we note that even the lowest concentrations of free amphiphile correspond to the transition A of Figure 3. At the transition itself the polymer collapses, and all new amphiphile is uti-

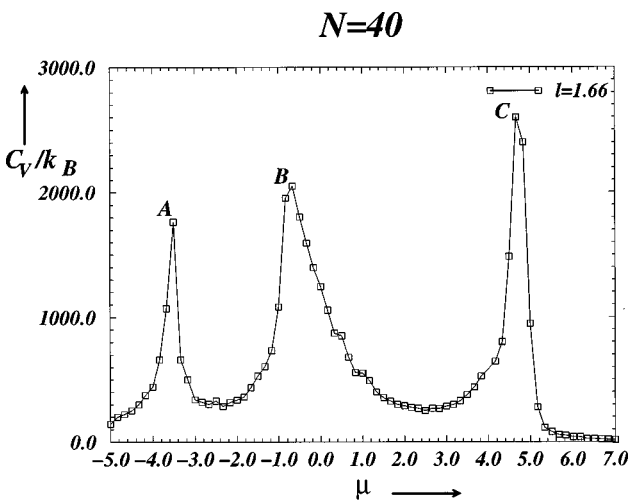

FIG. 7. Plot of the heat capacity, C_V/k_B, versus μ for $N=40$, $l=1.66(\square)$. A similar heat capacity plot is obtained for $l=5.0$. Appropriate extension of the simulation times have been used to generate these data.

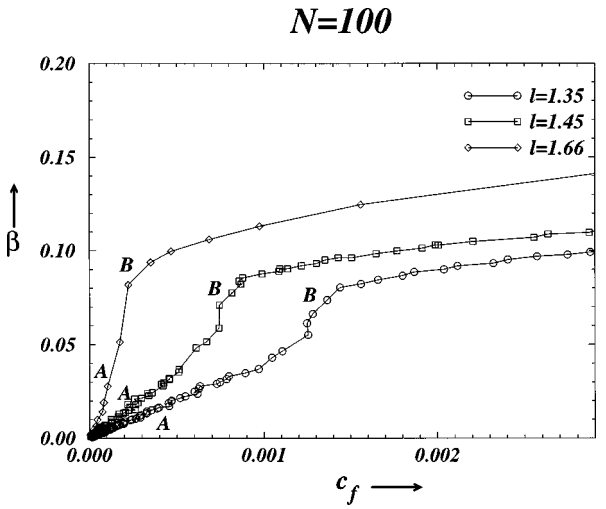

FIG. 9. Plot of the amphiphile-polymer binding curves, β versus c_f, for $N=100$, $l=1.35(\bigcirc)$, $l=1.45(\square)$, $l=1.66(\diamond)$, where A and B correspond to peaks in the heat capacity for the same parameters.

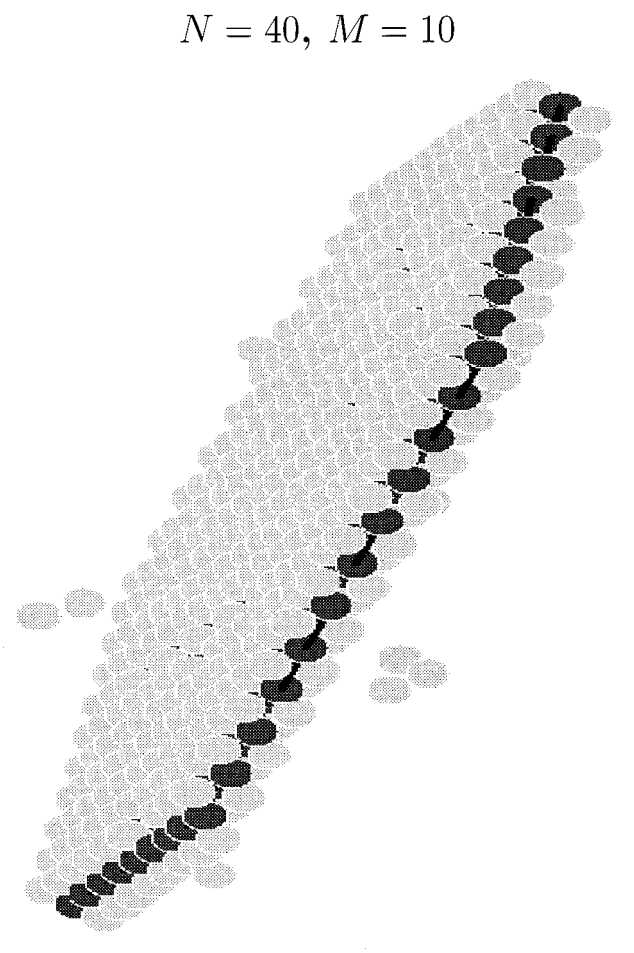

FIG. 10. Visual representation of a macroscopic self-assembled layered phase for a multi-polymer regime of M polymer chains, where $M=10$, $N=40$ and $l=1.66$. Solvent (white), amphiphile (gray) and polymer (dark gray/black).

lized to produce the collapse phenomenon. In Figure 8, we have marked the locations of the A and B transitions. Note that there is essentially no signature of the B transition for short polymer chains. When we turn to Figure 9, which illustrates a comparable range of parameters for $N=100$, we find that the A transition is reflected in β in a manner similar to that in short chain polymers. However, the B transition, where the polymer *platelet* is disrupted, and more of the polymer becomes available for binding is marked by a precipitous rise in β for $N=100$. Thereafter for $N=100$, saturation again occurs, as for short chain lengths.

Finally, we turn to a brief discussion of a somewhat more concentrated polymer regime. Thus we have considered a lattice containing ten chains, $M=10$ or $\phi_c=10/(20)^3$ for a variety of couplings. It is interesting to note that, for $l=1.66$, $N=40$, and $\phi_c=10/(20)^3$, there are analogous peaks A, B, C in the heat capacity to those for single polymers in Figure 7. However, the most remarkable and striking observation from the preliminary studies is that, for these polymer concentrations, the analogue of isolated polymer *platelet* formation (beyond peak A in Figure 5) is a macroscopic self-assembled layered phase illustrated in Figure 10. This is essentially in polymer liquid crystal phase.

IV. CONCLUSION

Our overall conclusion is that it is feasible to study a polymer-amphiphile-water lattice model using a combination of Monte Carlo moves that sample a wide variety of configuration space. In particular we have noted that reptations are helpful for even dilute polymer solutions, but essential for more dense amphiphile systems. We have also noted that even with a minimal set of interactions, albeit consistent with the most elementary properties of amphiphiles and polymers, a non-trivial phase diagram emerges. While some of the phenomena such as amphiphile-induced polymer collapse are observed in experiment, we have not yet attempted to make firm connection to typical phase diagrams. Rather we have emphasized the remarkably subtle interplay between microscopic interactions, entropy and concentration constraints that lead to conformational transitions at low polymer concentrations. The picture is even less clear at larger polymer concentrations, but it is evident that a whole new range of phenomena will emerge there. In particular we have noted the emergence of new classes of lamellar liquid crystalline phases where the polymers are effectively confined to layers by the amphiphile induced effective interactions. This is a matter to which we, and perhaps others, will return in future work.

ACKNOWLEDGMENTS

The authors would like to acknowledge interesting discussions with Professor P. G. de Gennes, Professor B. Widom and Dr. A. Berera. In particular we would like to thank our colleagues Alan Byrne for numerous fruitful discussions, David Hegarty and Paul Kiernan for advice on computer problems and Dr. A. Gorelov for helpful discussions of experimental work. The authors acknowledge the support of the Centre for High Performance Computing Applications, University College Dublin, Ireland. We would also like to thank the DEC Corporation for hardware support, and Fobairt for financial support.

[1] G. Gompper and M. S. Schick, Chem. Phys. Lett. **163**, 475 (1989).
[2] M. W. Matsen and D. E. Sullivan, Phys. Rev. A **41**, 2021 (1990).
[3] K. A. Dawson and Z. Kurtović, J. Chem. Phys. **92**, 5473 (1990).
[4] F. A. M. Leermakers and J. M. H. Scheutjens, J. Collid Interface Sci. **136**, 231 (1990).
[5] B. Widom, J. Chem. Phys. **84**, 6943 (1986).
[6] B. Widom, J. Chem. Phys. **90**, 2437 (1989).
[7] K. A. Dawson, Phys. Rev. A **35**, 1766 (1987).
[8] G. Gompper and M. Schick, in *Phase Transitions and Critical Phenomena*, edited by C. Domb and J. L. Lebowitz (Academic, London, 1994), Vol. 16.
[9] B. M. Knickerbocker, C. V. Pesheck, H. T. Davis, and L. E. Scriven, J. Phys. Chem. **86**, 393 (1982).
[10] N. Nishikido, J. Colloid Interface Sci. **136**, 231 (1990).
[11] M. Kahlweit *et al.*, J. Chem. Phys. **95**, 2842 (1991).
[12] G. Gompper and M. Schick, Phys. Rev. B **41**, 9148 (1990).
[13] K. A. Dawson, B. L. Walker, and A. Berera, Physica A **165**, 320 (1990).
[14] M. Laradji, H. Guo, and M. Zuckermann, J. Phys.: Condens. Matter **6**, 2799 (1994).
[15] D. Stauffer *et al.*, J. Chem. Phys. **100**, 6934 (1994).

[16] A. Mackie, K. Onur, and A. Panagiotopoulos, J. Chem. Phys. **104**, 3718 (1996).
[17] C. M. Wijmans and P. Linse, Langmuir **11**, 3748 (1995).
[18] M. Blume and D. Mukamel, Phys. Rev. A **10**, 610 (1974).
[19] M. Schick and W.-H. Shih, Phys. Rev. Lett. **59**, 1205 (1987).
[20] K. A. Dawson, M. D. Lipkin, and B. Widom, J. Chem. Phys. **88**, 5149 (1988).
[21] C. Buzano and L. R. Evangelista, J. Phys.: Condens. Matter **6**, 5323 (1994).
[22] A. Moskalenko and K. Dawson, J. Chem. Phys. **102**, 8201 (1995).
[23] H.-J. Woo, C. Carraro, and D. Chandler, Phys. Rev. E **52**, 6497 (1995).
[24] M. Kahlweit, R. Stry, and G. Busse, J. Phys. Chem. **94**, 3881 (1990).
[25] S. Komura *et al.*, J. Chem. Phys. **105**, 3264 (1996).
[26] F. Mallamace, N. Micali, and S. Chen, Physica A **1–2**, 170 (1996).
[27] P. J. Flory, in *Principles of Polymer Chemistry* (Cornell University Press, Ithaca, NY, 1953), Chaps. 12 and 13.
[28] P. G. de Gennes, *Scaling Concepts in Polymer Physics*, 3rd ed. (Cornell University Press, Ithaca, NY, 1988).
[29] Y. A. Kuznetsov, E. G. Timoshenko, and K. A. Dawson, J. Chem. Phys. **103**, 4807 (1995).
[30] E. G. Timoshenko, Y. A. Kuznetsov, and K. A. Dawson, Phys. Rev. E **53**, 3886 (1996).
[31] K. Zhang, G. Karlstrom, and B. Lindman, J. Phys. Chem. **98**, 4411 (1994).
[32] T. P. Lodge and M. Muthukumar, J. Phys. Chem. **100**, 13275 (1996).
[33] L. Piculell and B. Lindman, Adv. Colloid Interface Sci. **41**, 149 (1992).
[34] K. Hristova and D. Needham, Macromolecules **28**, 991 (1995).
[35] K. Veggeland and S. Nilsson, Langmuir **11**, 1885 (1995).
[36] L. Piculell, K. Bergfeldt, and S. Gerdes, J. Phys. Chem. **100**, 3675 (1996).
[37] K. Bergfeldt and L. Piculell, J. Phys. Chem. **100**, 5935 (1996).
[38] Y. Li, D. M. Bloor, and E. Wyn-Jones, Langmuir **12**, 4476 (1996).
[39] W. Meier, Langmuir **12**, 1188 (1996).
[40] R. Walter *et al.*, Macromolecules **29**, 4019 (1996).
[41] J. Fundin, P. Hansson, W. Brown, and I. Lidegran, Macromolecules **30**, 1118 (1997).
[42] A. Delville, Chem. Phys. Lett. **118**, 617 (1985).
[43] F. Guillemet and L. Piculell, J. Phys. Chem. **99**, 9201 (1995).
[44] K. Thuresson, B. Nyström, G. Wang, and B. Lindman, Langmuir **11**, 3730 (1995).
[45] K. Inoue, T. Sekido, and T. Sano, Langmuir **12**, 4644 (1996).
[46] J. Kevelam, J. K. L. van Breemen, W. Blokzijl, and J. B. F. N. Engberts, Langmuir **12**, 4709 (1996).
[47] B. Magny, I. Iliopoulis, R. Zana, and R. Audebert, Langmuir **12**, 2616 (1996).
[48] E. D. Kudryashov, A. V. Gorelov, and K. A. Dawson, J. Phys. Chem. (in press).
[49] P. M. Claesson *et al.*, *The International Symposium on Colloids and Polymer Science* (Nagoya Institute of Technology, Nagoya, Japan, 1996).
[50] S. M. Mel'nikov, V. G. Sergeyev, and K. Yoshikawa, in Ref. 49.
[51] S. Shimabayashi, T. Uno, Y. Oouchi, and E. Komatsu, in Ref. 49.
[52] A. Y. Grosberg and A. R. Khokhlov, *Statistical Physics of Macromolecules* (AIP Press, New York, 1994).
[53] H. Gould and J. Tobochnik, *An Introduction to Computer Simulation Methods: Applications to Physical Systems* (Addison–Wesley, Reading, MA, 1988).
[54] B. Magny *et al.*, Prog. Colloid Polym. Sci. **89**, 118 (1992).
[55] O. Anthony and R. Zana, Langmuir **12**, 1967 (1996).
[56] O. Anthony and R. Zana, Langmuir **12**, 3590 (1996).
[57] N. Isogai, J. P. Gong, and Y. Osada, Macromolecules **29**, 6803 (1996).
[58] K. Thuresson, O. Söderman, P. Hansson, and G. Wang, J. Phys. Chem. **100**, 4909 (1996).
[59] O. Philippova, D. Hourdet, R. Audebert, and A. R. Khoklov, Macromolecules **29**, 2822 (1996).
[60] K. T. K. Shirama and N. Takisawa, Bull. Chem. Soc. Jpn. **60**, 43 (1987).
[61] J. P. S. K. Hayakawa and J. C. Kwak, Biophys. Chem. **17**, 175 (1983).
[62] I. Satake and J. T. Yang, Biopolymers **15**, 2263 (1976).
[63] G. Schwarz, Eur. J. Biochem. **12**, 442 (1970).
[64] S. M. Mel'nikov, V. G. Sergeyev, Y. S. Mel'nikova, and K. Yoshikawa, J. Chem. Soc. Faraday Trans. **93**, 283 (1997).